IJSGS

ISSN: 2488-9229
FEDERAL UNIVERSITY
GUSAU-NIGERIA

INTERNATIONAL JOURNAL OF SCIENCE FOR GLOBAL SUSTAINABILITY

Design, Construction and Evaluation of 5A AC-DC Portable Lead Acid Battery Charger with an Inbuilt Automatic Shut OFF

***Yahaya, YUSUF**[1] and **Hassan Nawawi, YAHYA**[2]

[1]Department of Physics Zamfara College of Arts and Science Gusau, Nigeria

[2]Department of Electrical / Electronics Usmanu Danfodio University Sokoto, Nigeria

Corresponding Authors Email Address & Phone No.: bazata70@gmail.com phone no. +2347034909425

Received on: March, 2020 **Revised and Accepted on:** June 2020 **Published on:** July 2020

ABSTRACT

Battery charger is a system that restores battery after being discharged. It is well known that battery can be destroyed for being discharged below its manufacturers specified discharge voltage limit, when left for some hours. A single switch fly back buck converter that enables battery charging from the alternating current (AC) supply is designed, and constructed. To prevent the battery from overcharging an automatic charge controller was added to the design. Size of the charger was minimised by designing it to operate at higher frequency. It has an input potential difference (PD) from 80 to 250 volt. The circuit components and other design materials were chosen based on their simplicity and availability in most of the electronics shops. Red light emitting diode (LED) is ON when the charger is connected to the mains supply while the green LED is ON when charging is cut OFF or completed. The design was first conducted on MULTISIM software to ascertain the working conditions of the circuits before the construction procedure. Performance analysis was carried out and found working appropriately.

Keywords: Alternating Current, Automatic Shut off, Buck Converter, Light Emitting Diode, Potential Difference

1.0 INTRODUCTION

Although a battery is called a '12 volt' battery, its voltage varies from about 12.6 volts down to 10 volts when discharging. It can also rise up to 15 or 16 volts during charging. It is very important, however, to limit the maximum battery voltage during charging otherwise the battery will be damaged. During charging the battery voltage should not exceed 13.8 volts for long periods and 14.4 volts for short periods. Odia and Okpor (2017) a battery charger or recharger is a device used to put energy into a secondary cell or rechargeable battery by forcing an electric current through it. Jessica (2019) Car's alternator is not designed to fully restore a depleted battery, but rather to maintain a healthy one. Udezue, *et al.,* (2016) Observed that irrespective of the level of discharge, most battery service centres often connect the batteries and allow them to charge without a means to automatically disconnect them when they are fully charged in order to prevent over-charge and possible explosion. Faithpraise, *et al* (2016) designed and constructed a battery charger with a control circuit to monitor and regulate the process of charging several batteries ranging from 4 volts to 12 volts, using a photovoltaic (PV) solar panel as the input source.

In this study single fly back buck converter circuit is designed for charging a storage lead acid battery from the (AC) mains power supply. To prevent the battery from being damaged due to overcharging an automatic charge control is added. Green LED indicator is ON to shows that the charging is completed. It is designed to operate from low voltage of 80 to 250 volt. Therefore, the user needs not to look for a voltage stabilizer.

2.0 THEORY

Switched mode Power Supply (SMPS) always provide a well regulated power to the load irrespective of the input variations. SMPS incorporates a Pass transistor that switches very fast

typically at 50 Hz and 1 MHz between the ON and OFF states (Selim, and Alan, 2003). The critical conduction mode of operation is proposed as the most effective one of the fly back type of switch mode power supply (Sagar and Mohammad, 2009). The input DC voltage of the full-bridge MOFET converter or the output of the full-bridge diode converter at the AC input is converted to another output DC voltage using the full-bridge MOSFET converter, the transformer, and the secondary full-bridge diode converter, which are simply referred to as the full-bridge DC-DC converter (Su-Han, *et al.*, 2014)

2.1 Fly Back Converter

Figure 2.2 shows a fly back converter circuit. When transistor Q_1 is ON, due to the winding polarities, the diode D_1 becomes reverse-biased. Therefore, transformer core flux increases linearly. When transistor Q_1 is turned OFF, energy stored in the core causes the current to flow in the secondary winding through the diode D_1 and flux decreases linearly. Output voltage is given by Equation 2.1

$$V_{out} = V_{in} * \frac{N_2}{N_1} * \frac{d}{1-d} \qquad 2.1$$

Where d is the duty cycle of the transistors and N_2/N_1 is the secondary-to-primary turns ratio of transformer

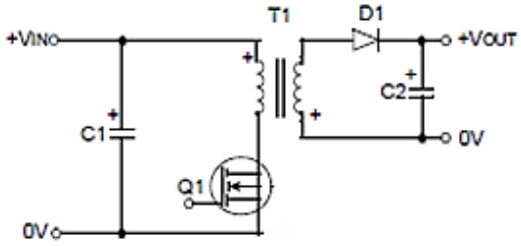

Sagar and Mohammad, (2009)

FIGURE: 2.2 A Fly back Converter

Power requirement in this work is not much hence the Fly back topology was adapted.

3.0 MATERILS AND METHOD

3.1 Circuit Design

The general block diagram of the system is as shown in Figure 3.1. The stages include input rectifier, oscillator, buck converter circuit, charge control and feedback voltage control. The circuit diagram prepared and simulated in NI MULTISIM to check if it works as expected.

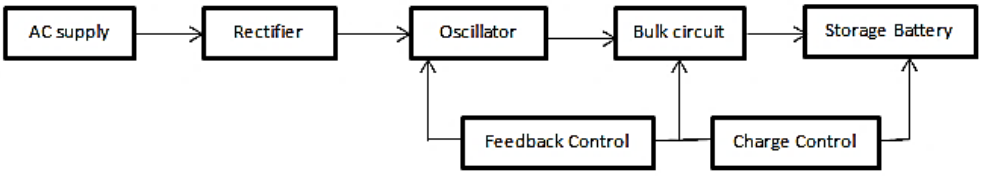

Figure: 3.1 General block diagram

3.2 Choice of Switch Oscillator

The integrated circuit (IC) used in pulse generator (oscillator) circuit is the KA3842. It is chosen due to its simplicity and availability. It has a low start up current, temperature compensated reference, high gain error amplifier, current sensing comparator, and high current totem pole output for driving a power MOSFET (KA3842 datasheet, 2015).The first step in selecting the oscillator components is to determine the required circuit dead time. Once obtained, is used to pinpoint the nearest standard value of timing capacitor (C_T) for a given dead time. The timing resistor (R_T) was calculated from the following expression;

$$F_{osc} = \frac{1.72}{R_T(k)C_T(uF)} \quad 3.1$$

Where; $F_{osc}$is the frequency of the oscillator, (R_T) is the timing resistor and C_T is the timing capacitor (UC3842 datasheet, 2015). C_T was kept at 4.7 nF and the frequency of the oscillator was chosen at 60 kHz. Equation 3.1 shows that R_T to be 6.1 KΩ, but 5.6 kΩ is closer standard value and therefore used. With the IC start-up current of 0.45 mA, a potential difference is established between the input DC source and that of the IC through a resistor R_{IN} (R_4). When V_{IN} is at low line (80 V), R_{IN} was found to be 178 kΩ, but 200 kΩ is been used. Ceramic monolithic bypass capacitors (0.1 pF) from V_{CC} and V_{REF} to ground provide low-impedance paths for high frequency transients at those points.

Since the KA3843 series has only a single output, it can drive the high voltage MOSFET transistor. The transistor chosen for this operation is UTC 10N40. The MOSFET has high switching speed, and $R_{DS(ON)}$ of 0.65Ω at V_{GS} of 10 Volt (UTC 10N40 Datasheet, 2016). Pin 3 of the IC is the current sense and this pin is connected to the sense pin of the power MOSFET. The circuit usually samples the voltage drop across a resistor in series with switching FET transistor. If the current rises abnormally due to some shorted circuit in the secondary side such as shorted secondary diode or horizontal output transformer hot, the voltage will exceed the reference level and shutdown the pulse generator.

3.3 High Frequency Transformer Design

The power source for the converter is the AC 220 V mains, and RMS, 311 V peak, at frequency of 60 kHz. For the charge to be potable the ferrite transformer was assumed to be 70 W, which is enough to provide the require charging current. The final output voltage of the charger is expected to be about 13.8 Volt. The selected core is Manganese Zinc, E130. Since the input PD is in range 80 to 230 V while the output voltage expected stay fixed due to feedback circuitry.

$V_{in(min)}$ = 80 V AC = (80 √2) V DC = 113 V DC, $V_{in(max)}$ = 230 V AC = (230 √2) V DC = 325 VDC, and $V_{in(nom)}$ = 160 V AC = (160 √2) V DC = 226 VDC From Faraday's Law;

$$V = 4.44NA_efB10^{-8} \quad 3.2$$

Where; *V* is the applied potential (volts RMS), 4.44 is the form factor for a sine wave, N is the number of turns, *A* is the core cross-sectional area (cm^2), f is the frequency (hertz), and B is the peak flux density (gauss).

The great benefit of ferrites, of course, is that they permit operation at frequencies into the hundreds of kilohertz, even to several megahertz. With the frequency very high, A and N may be set to small values, and the resulting magnetic is miniature in comparison with a low frequency device (Butler Technical bulletin, 2012. ON Semiconductor, (2005) the number of required primary turns is calculated from equation 3.3 that is;

$$N_{pri} = \frac{V_{in(nom)} * 10^8}{4.*f*B_{max}* A_c} \quad 3.3$$

Where: N_{pri} is the Number of Required Primary Turns, $V_{in\,(}$nom) is Nominal Input Voltage and A_c = A_e is Effective Cross-Sectional Area of the core in cm^2. The Maximum flux density (B_{max}) is taken to be in the range 1300G to 2000G. This will be acceptable for most transformer cores (Majid, 2009)

The oscillator's operating frequency was already chosen to be 60 kHz, while B_{max} was assumed to be 1500G. For TDK 47E (E130), the effective cross-sectional area given in the datasheet/specification sheet is 111 mm^2. To the nearest whole number n_{pri} was found to be 40 turns. The transformer output has to be greater than 13.8 V, due to voltage drop across the output rectifiers. Therefore, the transformer output must be [13.8 + (Total Voltage Drop Due to rectifier Diodes)] at all input voltages. Hence, transformer output was rated at 15.8 V to compensate for this drop. To allow gab for the dead time, the Pulse Width Modulation (PWM) controller was chosen to be 98% maximum duty cycle. At a maximum duty cycle of 98%, the average voltage to transformer is 0.98 * 160 V = 156.8 V. The ratio of primary to secondary is 156.8V/ $\sqrt{2}$ ∗15.8 V = 6.94, which is the turns ratio (N). Therefore; N_{sec} = N_{pri} / N = 40 / 6.94 is approximately 6 turns. Axillary winding was made to tally with that of secondary. Feedback is implemented to keep the output voltage fixed with line and load variations – changes due to

mains voltage or load. The TL431 and EL817 components were used for this function. EL817 photocoupler is used as a link between high and low voltages. The device was programmed with two external resistors; R_1 and R_2 (TL431 datasheet, 2015). The total dynamic impedance of the circuit was defined as:

$$|Z_{KA}'| = |Z_{KA}|(1 + \frac{R_1}{R_2}) \quad 3.4$$

Where Z_{KA} is the dynamic impedance, for the output voltage to be variable, the programmable external resistor (R_2) was replaced by a potentiometer. In single switch fly back an overvoltage spike is applied across the power switch each turn off. It was limited by introducing diode, capacitor and resistor (D-R-C) snubber circuit.

3.4 Charge Control Circuit Design

The circuit is to protect the battery overcharge, therefore prevent it from damage when left ON for long period. The design incorporated a relay circuit that cut OFF when the battery voltage rises to 13.5 Voltage. Red LED indicator shows that charging is ON, while green LED is ON when the battery is fully charged. The switching method employed two similar NPN transistors Q_1 and Q_2. For Q_2 to derive a coil relay, it was ensured that the maximum collector current (I_c) is greater than the load current. The transistor is biased so that the maximum amount of base current is applied, resulting in maximum collector current. This causes the minimum collector emitter voltage to drop as a result in the depletion layer being as small as possible and maximum current flow through the transistor. Therefore, the transistor is switched "Fully-ON". When using the transistor as a switch, a small base current controls a much larger collector load current

That is $I_c(max) > \frac{supply\ voltage(Vc)}{load\ resistance(RL)}$ 3.5

In actual practice, it is better to calculate about 30% more current than needed to guarantee our transistor switch is always saturated (Martell, 2014)

In this case, it was assumed that 180 mA is needed to drive the load (relay) and the applied potential difference (PD) is 13.5 V. 2N2222N datasheet, (2013) the 2N2222N transistor is a high speed switching application at collector current up to 500mA, and feature useful current gain over a wide range of collector current, low leakage currents and low saturation voltage, is also chosen. 1 mA was assumed to saturate Q_2 and Q_1 is design to operate at Quiescent Point,

The 5.0 kΩ potentiometer enabling cut OFF voltage to be setup. Martell, (2014) when using a transistor to turn on a relay coil, it is very important to use a 1N4001 diode reversed biased in parallel with the relay coil. This is to prevent the kickback voltage in the reverse polarity from destroying the transistor. The materials used in system construction were listed in table 3.0. The circuit diagram prepared with "National Instruments NI MUTISIM ", is presented in Figures 3.1

Table: 3.0 Lists of Components Used

S/N	Components	Description	Quantity
1	Diode	HFA25TB60	2
2	Rectifier Diode	SBR20A100CT	1
3	Zener	4.7 V	1
4	IC_1	TL431	1
5	IC_2	EL817	1
6	IC_3	KA3842	1
7	Ferrite Core	111 mm^2	1
8	MOSFET	10N40	1
9	Resistor	200 KΩ	1
10	Resistor	5.6 KΩ	1
11	Resistor	56 KΩ	1

12	Resistor	10 Ω	2
13	Resistor	10 KΩ	1
14	Resistor	1 Ω	1
15	Resistor	2.2 KΩ	1
16	Resistor	1 KΩ	3
17	Resistor	3.3 KΩ	1
18	Resistor	2.2 kΩ	1
19	Resistor	15 KΩ	1
20	Resistor	0.33 Ω	1
21	Capacitor	47 µf/400 V	1
22	Capacitor	0.1 µf	3
23	Capacitor	22 µf/50 V	1
24	Capacitor	47 nf	1
25	Capacitor	1nf	1
26	Capacitor	1000 µf/35 V	1
27	Potentiometer	5 kΩ	1
28	IC Socket	8 Pins	1
29	Coil Wire	28 Gauge	4 Meters
30	Coil Relay	12 V	1
31	LED	Green	1
32	LED	Red	1

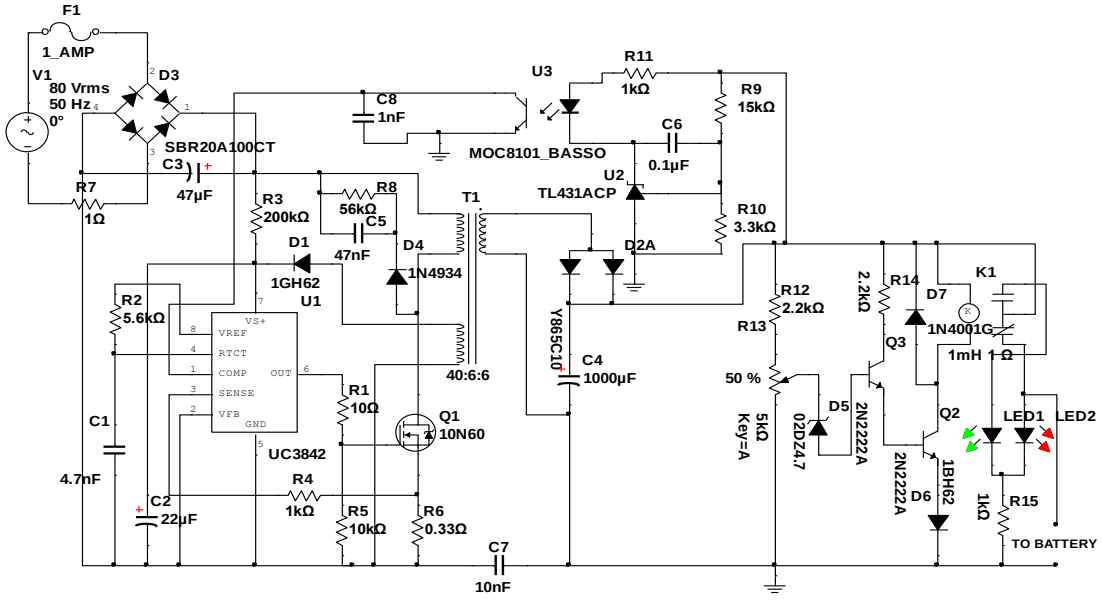

Figure: 3.2 Complete Circuit Design

3.5 System Construction

Multimeter was used to conduct a continuity test for the diodes, transistors and MOSFET. The resistors were also tested and found to be within their tolerance value. The conducting surfaces were sand papered to ensure cleaned surface and prevent dry joints during soldering. Continuity test was also conducted using the multimeter to ensure that the joints are properly done. During the soldering the active components were held by the pliers to help radiate the heat quickly. To prevent the UC3842 IC from damage due to overheating an IC socket was used as shown in plate (I)

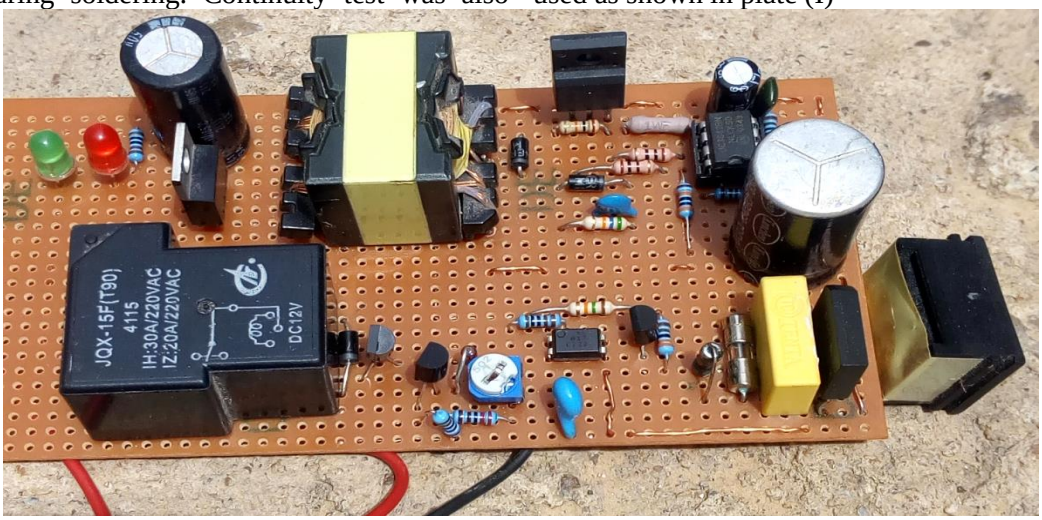

Plate: (I) Photograph of the constructed circuit

4.0 RESULTS AND DISCUSSION

4.1 Simulations Test Results

The simulation test was conducted at two points, the oscillator and the output stage of the charger circuit as shown in figure 3.1a and b

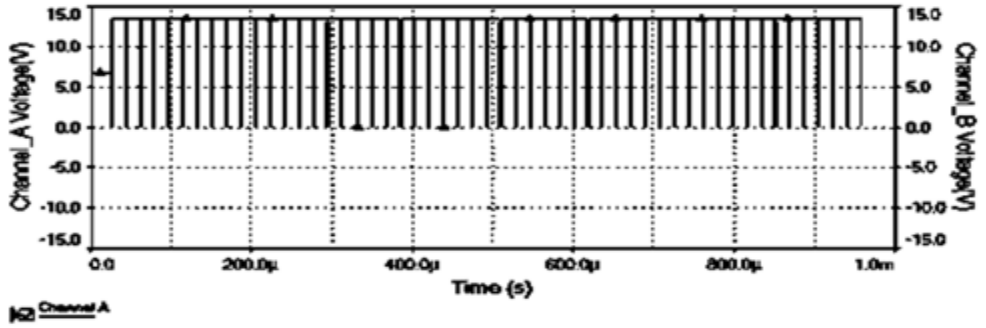

Figure: 3.1(a) Simulation Result of the oscillator Circuit in MULTISIM

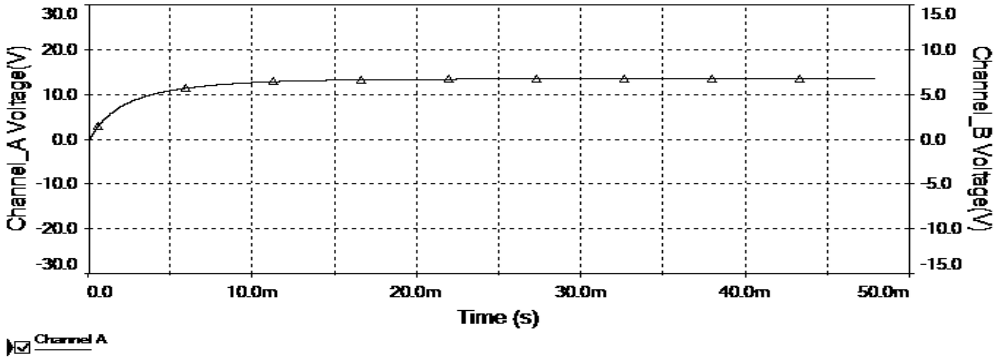

Figure: 3.1(b) Simulation Result of the output stage in MULTISIM

The result shows that the oscillator output is a square wave of high frequency. With C_t and R_t equal to 4.7 nF and R_t 5.6 kΩ the frequency at test point on the oscillator was found to be around 65 kHz with a very small variation of ± 0.4 kHz. Hence, the simulation results almost tally with the design. The charger output stage was found to be DC of about 18 Volt. The result shows that the circuit is working as estimated.

4.2 System Tests

After construction, the two sub circuits were tested to ascertain their working conditions. The oscillator was found to be operating at higher frequency of about 67 kHz, and the charger output to be 13.82 VDC when the input supply is between 80 and 250 volt. Test conducted on control stage shows a sharp cut OFF at 13.5 Volt. The next stage followed by connecting a discharged 7.2 A Lead acid battery of PD of about 10.40 V across the charger output terminals. A digital voltmeter was connected across the battery terminals and a digital ammeter in series to the charger circuit. The charger was put ON; the red LED indicator was ON showing that charging is in progress. After some time the green LED light ON, an indication that the charging was cut OFF. The PD across the battery terminals was measured and found to be 13.5 V. Current and voltage of the battery during charging was observed at timely intervals and presented as shown in figure 3.2a and 3.2b

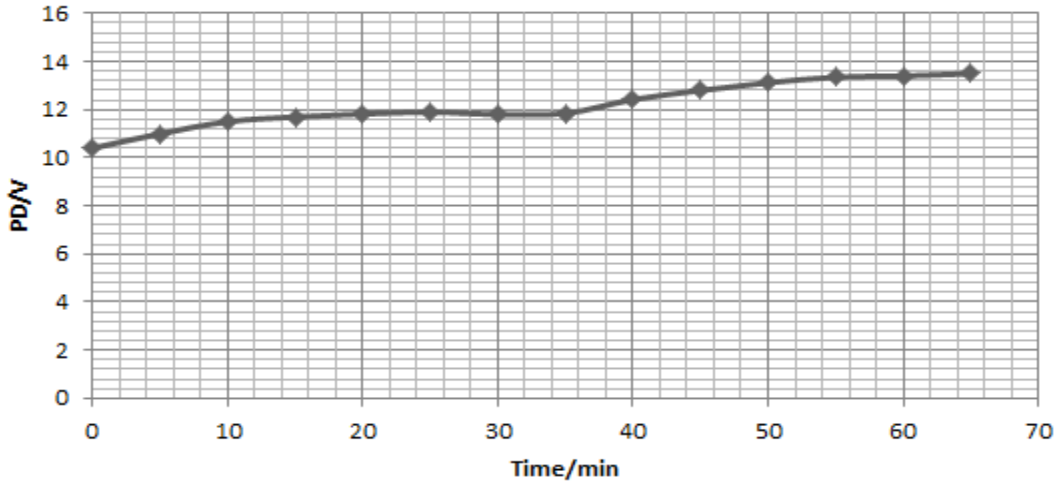

Figure 3.2a: Battery PD against Time

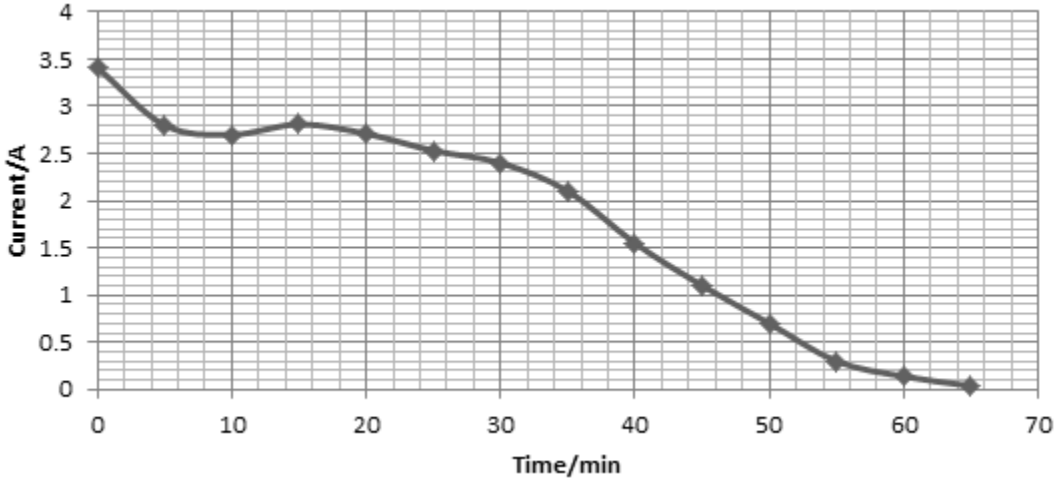

Figure 3.2b: Battery Charging Current VS Time

Figure 3.35a shows the battery PD gradually increases till it reaches 13.5 V though the variation is non- linear. While on the other hand, the current was depreciating non-linearly to zero (figure 3.2b). At this point the battery is said to be charged

5.0 CONCLUSION

The battery charger operates on input voltages ranging from 80 to 250 volt. Steady output of 13.8 VDC was obtained within the range. It is suitable for charging lead acid battery for cars and motorcycles. The maximum output current obtained was 5 amperes. From the test and analysis conducted the charger was found to be working satisfactory.

REFERENCES

2N2222 Datasheet, (2013). High Speed Switches, STMicroelectronics Components Industries, [Online] Retrieved April 12, 2015 from http://www.st.com

Butler Technical bulletin, (2012). Division of Spang and Company, PA 16003, [Online] Retrieved Mar 04 2013 from http://www.mag-inc.com

Faithpraise, F., Bassey, D., Charles, M., Osahon, O., Udoh, M., and Chatwin, C. (2016). Experimental Design and Construction of an Enhanced Solar Battery Charger. IOSR Journal of Electrical and Electronics Engineering, 11 (2). pp. 11-16. ISSN 2320-3331

Ferric Core Application Guideline. (2015). Ferrite Core for Switching Power Supplies, [Online] Retrieved Feb 17, 2015 from http://www.electronics-tutorials.ws/transistor/tran_1.html

Jessica, C. (2019). Importance of Car Battery Chargers, Batteries plus bulb, 2019 DURACELL Bethel CT 06801, [Online] Retrieved Nov 17, 2019 from https://www.batteriesplus.com/blog/power/importance-of-car-battery-charger

Majid, D. (9009). From Powder to Transformer, Fairchild Semiconductor Power Seminar (2008 – 2009) pp 2

Martell, M. (2014). Transistor as a Switch, Using Bipolar Transistors as Switches [Online] .Retrieved November 16, 2015, from http://www.calculatoredge.com

Odia O. O., and Okpor J. (2017) Design and Implementation of a Microcontroller-Based Adjustable Voltage Automatic Battery Charger, Nigerian Journal of Technology Vol. 36, No. 4, October 2017, pp. 1226–1232. Electronic ISSN: 2467-8821. http://dx.doi.org/10.4314/njt.v36i4.32

ON Semiconductor, (2005). Publication Order Number AND8039, Semiconductor Components Industries, LLC, [Online] Retrieved Jan, 3 201 from http://onsemi.com

Sagar, K., & Mohammad, K. (2009). Off line Reference Design Using the dsPIC Microchip Technology Incorporated, [Online] Retrieved Feb 2016 from www.microchip.com

Selim, G. M., and Alan, I. (2003). 250W Fly back SMPS Design for a Big Size CTV, IEEE Transactions on Consumer Electronics, Vol. 49 No. 4, Nov 2003 pg 912

Su-Han, K., Doo-Hee, Y., and Gang-Y, J. (2014). High-Efficiency AC-DC Switch-Mode Power Supply Using Full-Bridge Converter Circuits, International Journal of Control and Automation Vol.7, No.6 (2014), pp.189-200, [Online] Retrieved Jan 02, 2017 http://dx.doi.org/10.14257/ijca.2014.7.6.1

TL431 Datasheet, (2015). Programmable Precision Reference, ON Semiconductor Company, [Online] Retrieved Sep 05, 2015 from: http:// www.onsemi.com

UC3842 Datasheet, (2015) Low-Cost Current-Mode Control, Texas Instruments Incorporated, [Online] Retrieved May 15, 2016 from: http://www.ti.com

Udezue, CU., Eneh, J., Unachukwu A., Onyemelukwe I., and Onyeka, H. (2016). 12V Portable Battery Charging System, Pacific Journal of Science and Technology 17(1): 5-11. May 2016

UTC 10N40 Datasheet., (2016) -channel Power MOSFET, Unisonic Technologies Co., Ltd, N [Online] Retrieved Feb 17, 2017 from: http://www.unisonic.com.tw